Astron. Astrophys. 339, L41–L44 (1998)

ASTRONOMY AND ASTROPHYSICS

LETTER

Letter to the Editor

Discovery of a new 170 s X-ray pulsar 1SAX J1324.4–6200

L. Angelini[1,⋆], **M.J. Church**[2], **A.N. Parmar**[3], **M. Bałucińska-Church**[2], **and T. Mineo**[4]

[1] Laboratory for High Energy Astrophysics, Code 660.2, NASA/Goddard Space Flight Center, MD 20771, USA
[2] School of Physics and Astronomy, University of Birmingham, Birmingham, B15 2TT, UK
[3] Astrophysics Division, Space Science Department of ESA, ESTEC, Postbus 299, 2200 AG Noordwijk, The Netherlands
[4] Instituto IFCAI, via La Malfa 153, I-90146 Palermo, Italy

Received 31 August 1998 / Accepted 25 September 1998

Abstract. We report the discovery with BeppoSAX of a new 170.84 ± 0.04 s X-ray pulsar, 1SAX J1324.4−6200, found serendipitously in the field of the X-ray binary XB 1323−619 in 1997 August. The source and periodicity are also detected in archival ASCA data taken in 1994. The X-ray spectrum is modeled by a power-law with a photon index of 1.0 ± 0.4 and absorption of $(7.8 \pm^{2.7}_{1.1}) \times 10^{22}$ atom cm^{-2}. The source is located close to the galactic plane and within 3′ of the direction of the dark cloud DC 306.8+0.6. The measured interstellar absorption and cloud size imply a distance >3.4 kpc. This implies a 1–10 keV source luminosity of $>1.1 \times 10^{34}$ erg s^{-1} during the BeppoSAX observation. The source is not detected in earlier *Einstein* IPC and EXOSAT CMA observations, most probably due to reduced detector efficency and lower sensitivity to highly absorbed sources. The X-ray properties suggest that 1SAX J1324.4−6200 is an accreting neutron star with a Be star companion.

Key words: X-ray: stars – stars: rotation – pulsar: general – stars: individual: 1SAX J1324.4−6200

1. Observations

1.1. BeppoSAX

BeppoSAX (Boella et al. 1997) observed XB 1323−619, a low-mass X-ray binary (Parmar et al. 1998) between 1997 August 22 17:06 and August 24 02:02 UTC. The Narrow Field Instruments on BeppoSAX include the LECS (0.1–10 keV) and three MECS (1.8–10 keV) detectors, each at the focus of imaging telescopes. The fields of view (FOV) of the LECS and MECS are 37′ and 56′, respectively. The exposures in the LECS and MECS are 15 and 70 ks, respectively. Data from the MECS 2 and 3 (MECS1 failed in 1997 May) are summed. The MECS image, shown in Fig. 1, reveals in addition to XB 1323−619, the presence of 3 serendipitous sources. Sources A and J are 2E 1322.2−6157 and 2E 1325.5−6138, previously detected with the *Einstein* IPC (Parmar et al. 1989, P89). Of interest here is the new source located ∼17′ from XB 1323−619, with a count rate of $(1.86 \pm 0.07) \times 10^{-2}$ s^{-1}. The J2000 coordinates, derived from the MECS data, are R.A.=$13^{\rm h}\ 24^{\rm m}\ 26\overset{\rm s}{.}3$, Dec=$-62^\circ\ 00'\ 53''$ (galactic (l, b)= (306.793, 0.609)) with an uncertainty radius of $1\overset{'}{.}5$ (limited by the current uncertainty in the BeppoSAX position reconstruction for sources >10′ off-axis). We designate the source 1SAX J1324.4−6200. In the LECS the source is $16\overset{'}{.}7$ off-axis. Because of the smaller FOV a large fraction of the photons (∼75%) are lost on the detector wall. This, together with the reduced LECS exposure due to observational constraints, prevent the use of these data for spectral and timing analysis.

A total of 1940 MECS events within a radius of 4′ of 1SAX J1324.4−6200 were extracted. The arrival times were corrected to the solar system barycenter and binned with an integration time of 5 s. A single power spectrum (16384 frequencies) was calculated for the entire observation and is shown in Fig. 2. A strong peak is detected at 5.853×10^{-3} Hz (170.85 s) with a significance of $\sim 9\sigma$. No other peaks exceed the $\sim 3\sigma$ detection threshold. The period was refined by cross-correlating pulse profiles each obtained by folding data from 12 consecutive intervals. This yields a pulse period of 170.84 ± 0.04 s (at 90% confidence). The 1.8–10 keV pulse profile (Fig. 3) is approximately sinusoidal with a semi-amplitude (half of the peak to peak modulation divided by the mean count rate) of 52 ± 5%. The pulse shape and semi-amplidute do not show a strong energy dependence. The 4.5–10 keV/2.0–4.5 keV hardness ratio is constant, except for a slight hardening at Φ = 0.6–0.7 (where Φ = 0.0 is the intensity minimum). The lightcurve does not show eclipses, dips or strong variability with an upper limit of <14% *rms* at a binning of 400 s.

The MECS spectrum was rebinned to a minimum of 20 counts per bin, and was analyzed using an appropriate response matrix for the source position in the FOV. Due to the close proximity of the galactic ridge emission, a background spectrum was obtained from the same data using a source free region and the same extraction radius. A power-law model represents the data well with a χ^2 of 32 for 44 degrees of free-

Send offprint requests to: L. Angelini
⋆ Universities Space Research Association

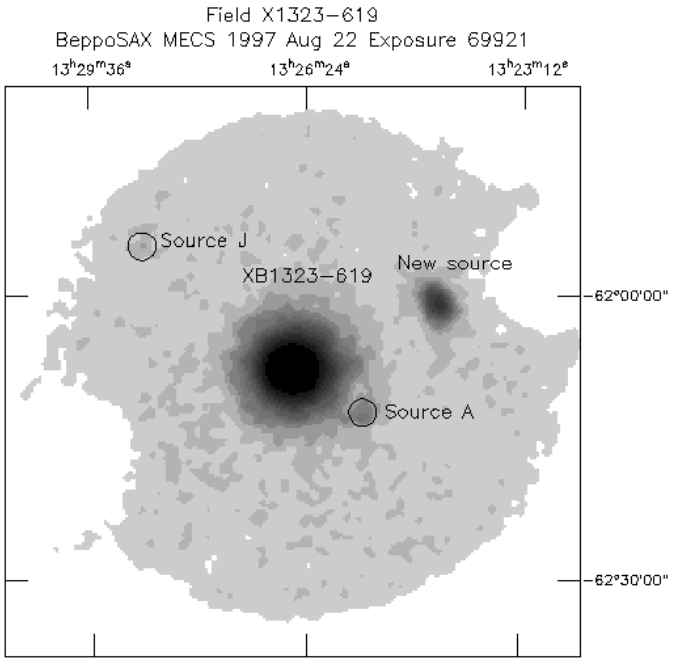

Fig. 1. The XB 1323−619 field MECS image (equinox J2000) smoothed with a Gaussian filter with a σ of 12″. The two "cut-outs" are due to the removal of calibration source events

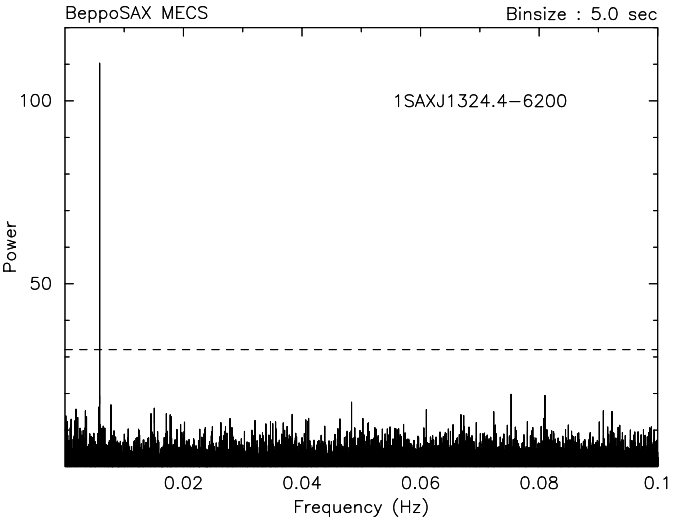

Fig. 2. The MECS 1.8–10 keV 1SAX J1324.4−6200 power spectrum. The dashed line indicates the 3σ threshold

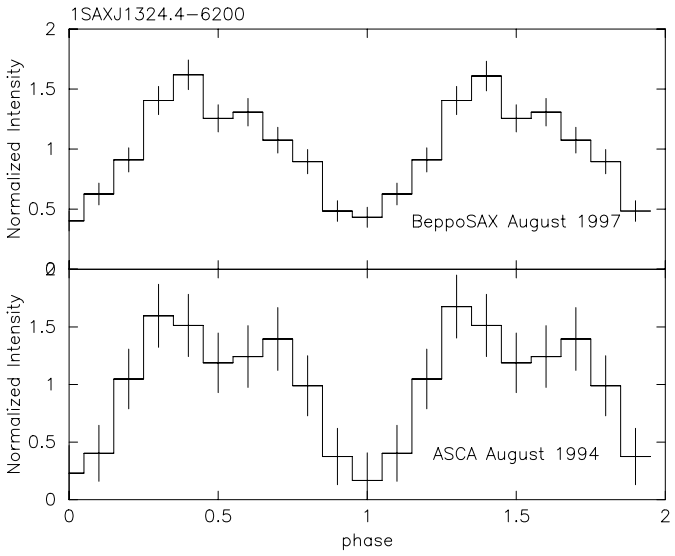

Fig. 3. Folded lightcurves at the best period for the BeppoSAX MECS (upper panel, 1.8–10 keV) and ASCA GIS (lower panel, 1.0–10 keV) data. Two cycles are shown

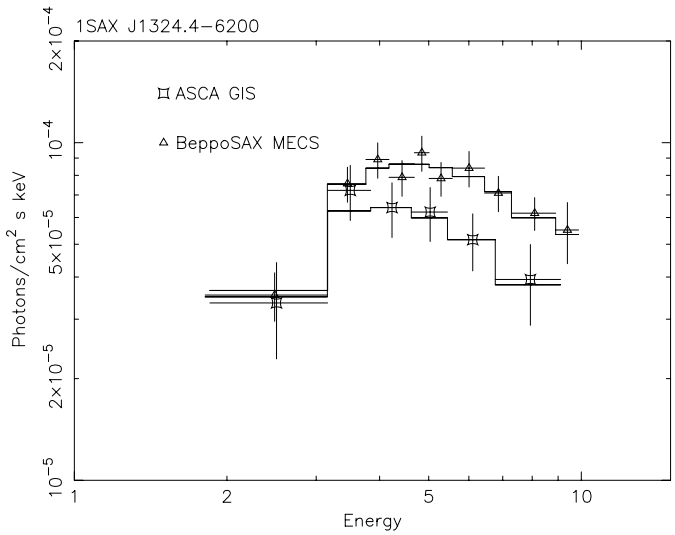

Fig. 4. MECS and GIS unfolded photon spectra. The solid line represents the best fit power-law model. Energy is in keV

dom (dof), with a photon index, α, of 1.0 ± 0.4 and absorption, N_H, of $(7.8\pm^{2.7}_{1.1}) \times 10^{22}$ atom cm^{-2} (Fig. 4). The 1–10 keV flux is 8.2×10^{-12} erg cm $^{-2}$ s^{-1}. No iron K line is detected with a 90% confidence upper limit of 98 eV to the equivalent width of a narrow line at 6.4 keV. Blackbody and bremsstrahlung models also fit the data. For a blackbody model, the temperature, kT, is 2.4 ± 0.4 keV and $N_H = (4\pm^{3}_{2}) \times 10^{22}$ atom cm^{-2}(χ^2/dof = 35/44). For a bremsstrahlung model, the temperature and absorption cannot be simultaneously constrained. The 90% confidence limit for kT is >10 keV and $(7.0 < N_H < 15.8) \times 10^{22}$ atom cm^{-2}. with a $\chi^2/dof \sim 1$. Although 1SAX J1324.4−6200 is in the FOV of the non-imaging HPGSPC (5–120 keV) and PDS (15–300 keV) detectors, no useful spectral or timing information could be extracted from these data. The folded lightcurves are consistent with a constant with a semi-amplitude of <62% (HPGSPC) and <10% (PDS) respectively. The observed counts are dominated by XB 1323−619 which is predicted to give 10 and 4 times more than 1SAX J1324.4−6200 in the HPGSPC and PDS respectively.

1.2. ASCA

ASCA (Tanaka et al. 1994) observed XB 1323−619 in 1994 August for a total of 20 ks. 1SAX J1324.4−6200 is detected

Table 1. Observations of 1SAX J1324.4−6200. C is count rate and θ off-axis angle. Upper limits are quoted at 3σ confidence. The MECS and GIS count rates are uncorrected for factor $\sim$2 vignetting, and θ is the average for each pair of units. The LECS count rate is affected by severe vignetting (see text)

Date (yr mn dy)	Instrument	Exp. (ks)	C (10^{-3} s^{-1})	θ ($'$)
83 Aug 20	*Einstein* IPC	4.5	$<$7.5	23.0
84 Feb 11	EXOSAT CMA	6.5	$<$3.3	9.5
85 Feb 11	EXOSAT CMA	93.7	$<$0.23	10.7
94 Aug 04	ASCA GIS(2,3)	19.4	22 ± 3	11.6
97 Aug 22	SAX LECS	14.9	5.1 ± 1.3	16.7
97 Aug 22	SAX MECS(2,3)	69.9	18.7 ± 0.7	15.5

in the GIS2 and GIS3 (0.8–10 keV) instruments (FOV $\sim$45$'$) at 12$'$.9 and 10$'$.3 off-axis, respectively. It is outside the 11$'$ (1 CCD mode) FOV of the SIS. The J2000 ASCA position is R.A.=$13^{\rm h}\ 24^{\rm m}\ 27\overset{\rm s}{.}6$, Dec=$-62^\circ\ 01'\ 41''$ (with an uncertainty radius of 1$'$.5), consistent with the MECS position. Photon event lists and spectra extracted from GIS2 and GIS3 were combined. The events were binned with an integration time of 5 s after barycentric correction. Power spectra of 4096 frequencies do not reveal significant peaks at the frequency of interest, with a limiting semi-amplitude $<$45%. A peak with a significance of 3.3σ is found at $\sim$170 s by searching with a folding technique in a small range of periods (155–185 s). Cross-correlating the mean pulses obtained from 5 intervals of the ASCA data gives a period of 170.35 ± 0.48 s. The 1.0–10 keV GIS pulse profile is similar to that obtained with the MECS (Fig. 3). A lower limit of the $|\dot{P}| < 1.0 \times 10^{-8}$ s s^{-1} is obtained combining the ASCA and BeppoSAX period measurements (using the lowest value allowed for the ASCA measurement). The lightcurve does not show significant variations with an upper limit of $<$15% *rms* at a binning of 400 s.

The combined GIS2 and GIS3 source spectrum was rebinned to have a minimum of 20 counts per bin. A power-law fit, using the appropriate off-axis response gives $\alpha = 1.3 \pm^{1.1}_{0.75}$ and $N_H = (6.6 \pm 2.5) \times 10^{22}$ atom cm^{-2} with a χ^2 of 27 for 34 dof, similar to the values obtained with the MECS. The 1–10 keV flux is 5.5×10^{-12} erg cm $^{-2}$ s^{-1}, $\sim$30% less than observed by BeppoSAX.

1.3. Earlier observations

Table 1 lists the 1SAX J1324.4−6200 count rates or upper limits for all available observations. The source was within the FOV of observations made with the *Einstein* IPC (0.4–4.5 keV) in 1983 and with the EXOSAT CMA (0.04–2 keV) in 1984 and 1985 (P89). It is not detected in any of these observations. The high absorption measured in the BeppoSAX and ASCA spectra means that the EXOSAT CMA non-detections are almost certainly due to the instrument's lower band pass and sensitivity. The predicted on-axis count rate of 3×10^{-6} s^{-1} is well below the upper limits given in Table 1. In the *Einstein* IPC observation, the pulsar was located at large off-axis angle, very close to a detector rib, at reduced detector efficency. Assuming the BeppoSAX spectral parameters, the expected on-axis count rate is 7.3×10^{-3} s^{-1}, consistent with the upper limit. The source is not included in the ROSAT all sky survey catalog (Voges et al. 1996), but the detection limit of 0.05 count s^{-1} is above the expected count rate of 5×10^{-4} s^{-1}. No counterpart was found by searching in the SIMBAD and HEASARC catalogs. 1SAX J1324.4−6200 lies in a very crowded region of the galactic plane. The digitized sky survey image contains more than 20 stars in the 1SAX J1324.4−6200 1$'$.5 radius position uncertainty circle, where the 10 brightest have a Vmag $\geq$13. These are unlikely to be the optical counterpart because of the high N_H inferred from the X-ray spectrum.

2. Source location

1SAX J1324.4−6200 lies within 3$'$ of the center of the dark cloud DC 306.8+0.6 (Hartley et al. 1986) which has an angular size of 6$'$. If 1SAX J1324.4−6200 is located behind the cloud a limit on the N_H and distance can be derived. Rowan-Robinson et al. (1991) present a simple relation to equate the IRAS 100 μm flux to the visual extinction, with an accuracy of $\pm$30% for 90% of sky. From the IRAS map at 100 μm, the flux at the source location is 725 MJy sr^{-1} which translates (using the above relation) to $N_H = 8.5 \times 10^{22}$ atom cm^{-2}. This value is consistent with the N_H measured from the X-ray spectra, giving a strong indication that the absorption measured in 1SAX J1324.4−6200 is not local to the system, but due to the dark cloud. Assuming the lower limit of the derived absorption and the average cloud density, as given in Stüwe (1990) of 3000 cm^{-3} for a single cloud, a cloud size of $\sim$6 pc is derived. This is intermediate between the average cloud size for dark cloud complexes (10 pc) and for simple dark clouds (1pc, Stüwe 1990). From the angular size of DC 306.8+0.6 and the above derived size, the distance to 1SAX J1324.4−6200 is estimated to be $>$3.4 kpc, giving unabsorbed 1–10 keV luminosities of $>1.1 \times 10^{34}$ and $>7.5 \times 10^{33}$ erg s^{-1} for the BeppoSAX and ASCA observations, respectively.

3. Discussion

The period and spectral properties of 1SAX J1324.4−6200 are common to both accreting magnetized neutron star X-ray pulsars (XRP) and accreting magnetized white dwarfs in intermediate polar (IP) systems. The limit on $|\dot{\rm P}| < 1.0 \times 10^{-8}$ s s^{-1} from these observations is insufficient to distinguish between neutron star and white dwarf models. If 1SAX J1324.4−6200 is an IP system in, or behind, the dark cloud DC 306.8+0.6, its luminosity is above the average of the short spin period (33–206 s) systems (Patterson 1994). This discrepancy could be resolved, if the measured absorption is local (other IP systems show high N_H) and the system closer. Patterson (1994) shows that if spin equilibrium is assumed for IP systems, then the magnetic moment and spin period are correlated. Assuming that the measured period is at equilibrium for a magnetic mo-

ment of $\mu = 2 \times 10^{32}$ G cm^{-3}, the luminosity derived using the Patterson (1994) relation is 1.3×10^{34} erg s^{-1}. This is above the range of $10^{31} - 4 \times 10^{33}$ erg s^{-1} expected for IP systems. Some IP such as GK Per (Watson et al. 1985) show outbursts with luminosities similar to 1SAX J1324.4−6200. However, it seems unlikely that the source was in outburst for the three years covered by the ASCA and BeppoSAX observations.

If 1SAX J1324.4−6200 is behind the dark cloud the measured luminosity is instead consistent with the XRP luminosity distribution ($10^{32} - 10^{38}$ erg s^{-1}). An equilibrium period of 170 s implies a magnetic field of $>3 \times 10^{12}$ G (Bildsten et al. 1997), which is within the expected range for XRP. The population of accretion-powered XRP has greatly increased, due to observations with the more sensitive detectors on ROSAT, ASCA, RXTE and BeppoSAX. Bildsten et al. (1997) list 44 X-ray pulsars and at least 6 others have been recently discovered (Israel et al. 1998; Kinugasa et al 1998; Corbet et al 1998; Marshall et al. 1998; Wijnands & van der Klis 1998; Hulleman et al. 1998). Most XRP are high-mass X-ray binaries (HMXRB) with five exceptions (4U 1626−67, Her X-1, GX1+4, GRO J1744−28, and SAX J1808.4−3658), which are low-mass systems. 1SAX J1324.4−6200 is unlikely to be one of the exceptions since they are more luminous and show different types of variability such as flares, bursting and transient behavior.

Roche-lobe filling (Cen X-3) and fed-wind supergiant (Vela X-1) HMXRB are the most luminous ($\sim 10^{35} - 10^{38}$ erg s^{-1}) XRPs. They shows marked X-ray intensity variability, due either to eclipses or to inhomogeneities in the companion's wind. Unless both X-ray observations took place during unusually low states of 1SAX J1324.4−6200, a supergiant companion seems unlikely because of the low luminosity and lack of variability. More than half of the HMXRB are associated with Be star companions and typically show transient behavior. This profusion of Be/X-ray pulsar systems is unsurprising. Van Paradjis & McClintock (1995) predict a ratio ∼100 of Be/X-ray binaries to HMXRB with evolved companions. Therefore many more Be/X-ray binaries are likely to be discovered in galactic plane surveys by ASCA and BeppoSAX. The luminosity of Be-star systems during outbursts can change dramatically from 10^{33} to 10^{38} erg s^{-1}, whereas persistent Be system such as X Per, or Be systems in quiescence, have more modest luminosities of $\sim 10^{33} - 10^{35}$ erg s^{-1}, similar to 1SAX J1324.4−6200. X Per (e.g. Schlegel et al. 1993) and 1SAX J1324.4−6200 have similar overall spectral shapes and neither show strong energy-dependent pulse profiles nor evidence for Fe K line emission. Be/X-ray systems display a correlation between their spin and orbital periods (Corbet 1986; Bildsten et al. 1997) which implies an orbital period of $\gtrsim$100 days for 1SAX J1324.4−6200. While 1SAX J1324.4−6200 is more likely to host a neutron star than a white dwarf, a change in the spin period of $|\dot{\mathrm{P}}/\mathrm{P}| \sim 10^{-4}$ yr^{-1} (similar to X Per, Haberl 1994), expected because of the lower moment of inertia of a neutron star, is needed to confirm this.

Acknowledgements. The BeppoSAX satellite is a joint Italian-Dutch programme. We thank the staff of the BeppoSAX SDC for help with these observations. This research has made use of the HEASARC archive, provided by NASA's GSFC.

References

Boella G., Butler R.C., Perola G.C., et al., 1997, A&AS 122, 299
Bildsten L., Chakrabarty D., Chiu J., et al., 1997, ApJS 113, 367
Corbet R.H.D., 1986, MNRAS 220, 1047
Corbet R.H.D., Marshall F.E., Lochner J.C., et al., 1998, IAU Circ. 6803
Haberl F., 1994, A&A 283, 175
Hartley M., Manchester R.N., Smith R.M., et al., 1986, A&AS 63, 27
Hulleman F., in 't Zand J.J.M., Heise J., 1998, A&A 337, L21
Israel G.L., Angelini L., Stella L., et al., 1998, MNRAS, 298, 502.
Kinugasa K., Torii K., Hashimoto Y., et al., 1998, ApJ 495, 435
Marshall F., Gotthelf E.V., Zhang W., et al., 1998, ApJ 499, L179
Parmar A.N., Gottwald M., van der Klis M., van Paradijs J., 1989, ApJ 338, 1024
Parmar A.N., Bałucińska-Church M., Church M.J. et al., 1998, in preparation
Patterson J., 1994, PASP 106, 209
Rowan-Robinson M., Hughes J., Jones M., et al., 1991, MNRAS 249, 729
Schlegel E.M., Serlemitsos P.J., Jahoda K., et al., 1993 ApJ 407, 744
Stüwe J.A., 1990, A&A 237, 178
Tanaka Y., Inoue H., Holt S.S., 1994, PASP 46, L37
Van Paradijs J., McClintock J.E., 1995, In: Lewin W.H.G., van den Heuvel E.P.J., van Paradijs J. (eds.) X-ray Binaries. Cambridge Astrophysics Series 26, p. 1
Voges W., Aschenbach B., Boller Th., et al., 1996, IAU Circ. 6420
Watson M.G., King A.R., Osborne J., 1985, MNRAS 212, 917
Wijnands R., van der Klis M., 1998, Nat 394, 344